Coupled numerical and experimental analyses of load transfer mechanisms in granular-reinforced platform overlying cavities

Caroline Chalak, Laurent Briançon, Pascal Villard

Coupled numerical and experimental analyses of load transfer mechanisms in granular-reinforced platform overlying cavities

Caroline Chalak[a,*], Laurent Briançon[a], Pascal Villard[b]

[a] Université de Lyon, INSA-Lyon, GEOMAS, 34 Avenue des Arts 69621, Villeurbanne Cedex, France
[b] Univ. Grenoble Alpes, CNRS, Grenoble INP, 3SR, 38000, Grenoble, France

A numerical model based on Finite Element Method (FEM) - Discrete Element Method (DEM) coupling is used to reproduce well controlled laboratory experiments that simulate circular cavity openings under granular em-bankments reinforced by a geotextile. The numerical deflection of the geotextile, the surface settlement and the soil expansion factor were investigated for various embankment heights, diameter ratios, cavity-opening modes, soil properties, and geotextile stiffnesses, and then compared to the results of laboratory tests. The load transfer mechanisms were also investigated. Good agreement between numerical and experimental results is shown, thus demonstrating the relevance of the numerical model. Complementary to the experiments, a numerical sensitivity analysis, that allows highlighting the influence of the main parameters and improving experimental observation, was also performed.

1. Introduction

The presence of opening of underground cavities in railway and highway applications is a major concern in civil engineering. To avoid the collapse of such structures, reinforcement methods such as nails, piles, and geosynthetics are employed.

The use of geosynthetics is quite popular among reinforcement techniques as it is an economical solution that saves time with moderate costs. It is also easy to install and has limited environmental impact. The geometry, size, and evolutionary opening mode of these cavities depend strongly on the geological context and on the nature of soil of the embankment. This makes understanding the collapse mechanisms in these structures overlying cavities a complex task and spotlights the difficulties in developing a proper design technique. The actual design methods are based on many assumptions that need to be improved to better reflect the real mechanisms that develop in the granular em-bankments, especially in the expansion of the granular soil over the cavity and the load transfer mechanisms that have considerable influence on surface settlement. To highlight the understanding of such mechanisms and to set bases to improve existing design methods, a numerical tool (SDEC- Spherical Discrete Element Code) originally developed by Donzé and Magnier (1995), improved by Le Hello (2007) and Villard et al. (2009) was used to analyze at the local scale the interactions between all the components of the reinforced structure during the opening of the cavity. To fulfill this goal, the numerical model appears to be a relevant tool that allows for definition of the contact forces between soil particles characteristic of the load transfer mechanisms and the vertical forces acting on the geosynthetic (over the cavity, at the vicinity of the cavity, and on the surrounding areas). In this paper the numerical model was confronted to laboratory experiments performed to highlight physical phenomenon that were observed at the field scale but not demonstrated due the difficulties to access to precise experimental data. The confrontation between the numerical model and the experiments carried out for the same purpose allows to give relevant conclusions about the influence of embankment thickness, the geotextile stiffness, and the opening cavity mode on the load transfer mechanism and the soil surface settlement.

2. Background

Many experimental studies have investigated the load transfer mechanisms within reinforced geosynthetic embankments overlying an open cavity. Full-scale experiments were performed (Alexiew, 1997; Blivet et al., 2000; Kinney, 1986; Kinney and Connor, 1987, 1990; Villard et al., 2000) to understand the reinforcing mechanisms and to improve the design methods. In France, project RAFAEL (Villard et al., 2000) highlighted the influence on the arch mechanisms of the embankment soil characteristics, the height of the embankment (H), and

* Corresponding author.
E-mail addresses: caroline.chalak@insa-lyon.fr (C. Chalak), laurent.briancon@insa-lyon.fr (L. Briançon), pascal.villard@univ-grenoble-alpes.fr (P. Villard).

the *H/D* ratios (*D* is the cavity diameter). In Briançon et al. (2004, 2005), the influence on the surface settlement of the geosynthetic stretching and sliding was discussed.

True-scale experiments were performed in 2012 in the framework of the French research project GEOINOV using granular and cohesive materials. The instrumentation used made it possible to measure the surface settlement, geosynthetic strain, and vertical stresses acting near the cavity. Nevertheless, the influence of the thickness of the embankment, granular material properties, and tensile stiffness of the geotextile on the load transfer mechanisms and on the soil expansion phenomenon was not well established.

Laboratory experiments are an easier way to conduct such studies (Pham et al., 2018; Rui et al., 2016; Schwerdt et al., 2004b). Laboratory experiments that support the present numerical work (Pham et al., 2018), show the considerable influence of the opening mode (trapdoor or progressive opening by increasing the diameter) on the geometry of the load distribution acting on the geotextile and on its strain. The displacements within the granular embankment, the geotextile deflection, and the soil surface settlement were measured. The expansion factor (defined as the ratio between the final volume of the collapsed soil above the cavity over its initial volume) was also evaluated considering several H/D ratios, densities of the soil, geosynthetic stiffness, and cavity opening modes. The results mainly show that the expansion factor values used in the actual design methods underestimate those measured in the field, leading to higher safety.

On the other hand, Finite Element Method (FEM) and Discrete Element Method (DEM) models were also used to study the load transfers in granular embankments reinforced by geosynthetic and sited above a cavity. The FEM models used cable, beam, and plane elements often associated with shell elements to model the geosynthetic sheets. Important mechanisms such as the membrane behavior (to consider a large strain) and the nonlinear tensile behaviors of the geosynthetic and of specific reinforcement yarn directions were included in the work of Villard and Giraud (1998).

The main drawbacks of these models are linked to the difficulty in properly describing the granular nature of the soil and the interactions between the soil and the geosynthetic. DEM models are instead able to describe the discontinuities of the soil at the grain scale. The shape, size, rotations and rearrangement of the grains are easily considered. The geosynthetic sheet can be modeled using discrete elements joined together (Chareyre and Villard, 2005; Chen et al., 2012; McDowell et al., 2006). The main disadvantage of this method is that the roughness of the soil-geosynthetic interface depends on the relative sizes of the soil particles and geosynthetic elements and is modified during the stretching of the sheet by the increase in the gap between the discrete particles used to model the geosynthetic. A coupled FEM-DEM model (Villard et al., 2009) in which the geosynthetic is modeled in FEM (using thin triangular plane elements associated with each other to constitute a continuous sheet) and the soil in DEM can overcome the limitations described above.

In 2016, Villard et al. (2016) have used successfully this numerical tool to simulate full-scale experiments, thus highlighting the influence of the cavity-opening mode and the H/D ratio on the geosynthetic deflection and load transfer mechanisms. The geosynthetic deflection and surface settlement are compared to the experimental values, and thus the global expansion coefficient was calculated and found to be non-uniform within the granular embankment. The results also show that the load distribution on the geosynthetic sheet depends strongly on the cavity-opening mode, and that the intensity of the load transfer mechanism can be estimated by Terzaghi's formulation only if an adequate value of the coefficient *K* (defined by Terzaghi as the earth pressure coefficient) is used (K = 1.3) when considering H/D ratios between 0.25 and 2.

Finally, the current design methods consider that the geosynthetic behaves as a flexible membrane and develops tensile forces once strained. The friction between the embankment and geotextile, the expansion of the soil, and the load transfer in the granular embankment were roughly taken into account.

Consequently, these methods need to be improved as they are based on many simple assumptions:

- The assumed shape of the soil volume impacted by the opening of a cavity is considered cylindrical (RAFAEL Project) or truncated (British Standard, 2010). The latest laboratory experiment by Pham et al. (2018) show that the shape of the collapsed soil area above the cavity can be either cylindrical in the case of small deformations or conical when the deformations are higher. However, it is believed that the shape of the collapsed soil volume above the cavity depends also on many other factors such as the soil properties. This remains an open question for investigation.
- The arching effect (or, in other terms, the ability of the granular material to develop a load transfer in sheared zones submitted to significant relative displacements (Briançon and Villard, 2008)) is considered by means of shear lines sited on the sides of the collapsed zone (Terzaghi, 1943). This does not consider other factors such as the rotation of the principle stresses.
- The British method (British Standard, 2010) is based on two-dimensional analysis for isotropic geosynthetics (Giroud, 1995) and considers that the sheet is fixed on the edge of the cavity. It was shown in the works of Briançon and Villard (2008) and Villard and Briançon (2008) that there is sliding of the sheet in the anchorage areas, which leads to higher surface settlements. These mechanisms were recently considered in the French method “Renforcement de la base de remblai PRXPG38063” in 2018. The German method, however, EBGEO (2010) considers the isotropic or anisotropic nature of the geosynthetic following the principles of the method introduced by Schwerdt et al. (2004a).
- The load applied to the geosynthetic sheet is considered uniformly distributed above the cavity and in the anchorage areas (Briançon and Villard, 2008; Feng et al., 2017a; Villard et al., 2000). In fact, the load distribution is influenced by many factors (e.g., the geometry of the cavity, opening mode, loading type, and soil properties). Numerical simulations have shown that this assumption of a uniform load is not adequate above the cavity: for a progressive opening of the cavity by increasing its diameter, the load distribution is approximately conical, while it takes the shape of a rather inverted paraboloid in the case of a trapdoor opening (Villard et al., 2016). This was also validated by Pham et al. (2018).
- Several research studies consider that the expansion coefficient is uniform within the entire collapsed volume of soil above the cavity and can be defined as the ratio between the maximum deflection of the geotextile and the maximum value of the surface settlement considering a parabolic shape of both deformed areas. In fact, as demonstrated by Villard et al. (2016) and Pham et al. (2018), the shapes of surface settlement and geotextile deflection are not always parabolic, and the expansion coefficient is not uniform and depends both on the characteristics of the granular material and on the soil confining pressure or loading modes.

Thus, to improve the present knowledge, coupled numerical and experimental works were performed for the same purpose. The advantage of the numerical tool consists in its ability to analyze at the macroscale complex physical mechanisms involved that are not reasonably possible to determine from an experimental point of view. The present paper focuses on the comparison of the numerical results with the experimental ones of Pham et al. (2018) and on a sensitivity analysis of main parameters.

3. Experimental setup

This section summarizes the experiments presented by Pham et al. (2018), to which the numerical results are compared. The conducted

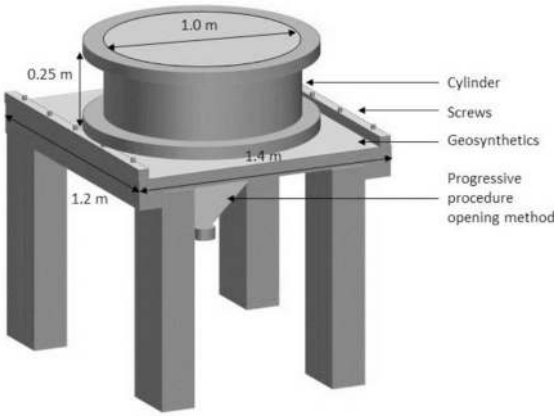

Fig. 1. Illustration of experimental device from Pham et al. (2018). 45.

laboratory experiments were developed to simulate collapses under a geosynthetic-reinforced platform. These experiments developed to simulate collapses under a geosynthetic-reinforced platform were carried out on fine sand (with elongated particles) considering two methods of cavity opening (trapdoor and progressive openings by an increase in cavity diameter), two types of geosynthetics (woven or nonwoven), and three different embankment heights (H/D = 0.5, 1, and 1.5).

The main experimental device consists of a rectangular table ($1.2\,m \times 1.4\,m$) connecting the test items. A 0.5-m-diameter round hole is located at the center of the table to simulate the cavity (Fig. 1). The geosynthetic sheet is stretched out and fixed on the table via screws and metallic clamps. The height of the platform varies by using one, two, or three metallic cylinders of $0.25\,m$ height each. The soil filling is done manually 10 kg by 10 kg with a bucket in a way to ensure a uniform soil density distribution ($\rho = 1.4\,Mg/m^3$). Each soil bucket was subsequently weighted. Moreover, in order to control the density of tested soils, a vibration tamper could be used. The surface soil was then flattened to avoid any confusion in the following analysis steps. The sand peak friction angle, obtained using triaxial tests performed at low confinement pressures, is equal to 36.5° when considering a relative density of the sand sample of 0.23. The geosynthetic fabrics were selected in order to respect similarity laws. The geosynthetic stiffnesses in the production and transverse directions were deduced from the tensile laboratory tests performed on the geosynthetic sheets. Actually, the low values of the vertical pressure acting on the geosynthetic during the cavity opening process and the slow rate of the cavity opening guarantee that the apparent stiffnesses of the geosynthetic during laboratory experiments are similar to those measured during the tensile tests.

The stiffnesses of the geosynthetics used in the experiments are as follows:

— Woven geotextile: Machine-direction stiffness: 160 kN/m; Cross-direction stiffness: 160 kN/m
— Nonwoven geotextile: Machine-direction stiffness: 9.21 kN/m; Cross-direction stiffness: 8.75 kN/m

To simulate the “trapdoor opening” mode of the cavity, a rigid circular plate, sited at the base of the granular layer, is moved vertically by the mean of a jack. For the “progressive opening” mode of the cavity by increasing its diameter, a cone filled with sand is gradually emptied to induce a concentric opening under the geosynthetic sheet. During the cavity-opening process, a laser sensor placed above the granular layer, then below the geosynthetic sheet, is used to measure the surface settlement and the geosynthetic deflection, respectively. To estimate the vertical stress distribution on the geotextile sheet, a tactile pressure sensor is used (a stretchable Tactaray system from PPS constituting by 512 sensors). The sensor is $0.32\,m$ long and $0.16\,m$ wide and was placed either over the cavity or at the anchorage areas (Pham et al., 2018).

4. Numerical model

4.1. Basic principles of FEM-DEM model

An FEM-DEM coupled model defined by Le Hello (2007) and Villard et al. (2009), in which the geosynthetic sheet is modeled using thin triangular elements (Villard and Giraud, 1998) and the soil using discrete elements is adopted in this study. The geosynthetic sheet is modeled using thin triangular elements, cylinders, and spheres (Villard and Giraud, 1998). The anisotropic fibrous behavior of the sheet is restored using different thread densities and various yarn stiffness values in each direction. The FEM element force-displacement relation established for each thread direction (Villard and Giraud, 1998) is a nonlinear function defined as follows:

$$\boldsymbol{F_e = K_e u_e + R_e} \tag{1}$$

Where K_e is the elementary rigidity matrix characteristic of one thread direction, u_e is the nodal displacement vector, and R_e is a vector taking into consideration high displacements. The entire rigidity matrix of one sheet element is equal to the sum of the elementary rigidity matrices. The DEM model used for the soil particles is based on the method developed by Cundall and Strack (1979). For two interacting grains, the contact is defined by normal and tangential stiffnesses and an intergranular friction angle. The relation between the contact force (divided into a normal and a tangential force by considering the plane that is tangent to the contact point) and the relative displacement is assumed to be linear elastic-plastic. The normal component of the contact force F_n is related to the normal overlaps u between the grains by the normal stiffness k_n, and the incremental tangential component of the force F_t is related to the incremental relative tangential displacement v by the tangential stiffness k_t of the contact.

The shear stiffness k_t is related to the normal stiffness through a coefficient α such as:

$$\boldsymbol{k_t = \alpha k_n} \tag{2}$$

The normal force acting on the interacting particles is:

$$\boldsymbol{F_n = k_n u \;\; if \;\; u \leq 0 \;\; else \;\; F_n = 0} \tag{3}$$

The increment of the tangential force is given as:

$$\boldsymbol{\Delta F_t = k_t \Delta v} \tag{4}$$

The interaction between the particles follows the Coulomb friction law. Thus, the tangential force is limited to a maximum absolute value of $|F_t| \leq F_n \tan\varphi_c$ (Fig. 2), where φ_c is the intergranular friction angle. The normal contact stiffness $_{kn}$ (or the tangential contact stiffness k_t) between two spheres of radius R_i and R_j, expressed in N/m, is defined as follows by a function of the normal rigidity K_{nij} (or the tangential rigidity K_{tij}) of the two constitutive materials of the spheres in contact, expressed in N/m^2:

$$k_n = \frac{K_{nij}(R_i * R_j)}{R_i + R_j} \tag{5}$$

For the application to sinkhole embankments, the main part of the soil deformation is plastic strains due to the large displacements and

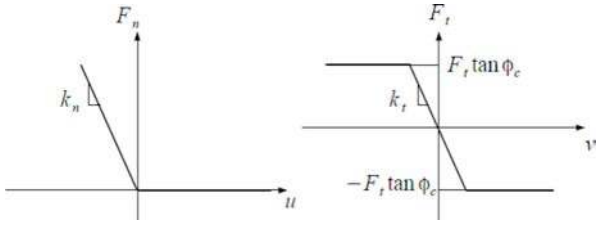

Fig. 2. Elastic contact law for normal interaction and elastic-plastic tangential interaction.

rotations of the grains during the opening process. Considering that the displacements due to the elasticity between grains can then be neglected and have no significant influence on the contact forces network and on the results, a basic linear elastic-plastic interaction law, keeping also a reasonable computational time, seems reasonably relevant.

The numerical procedure is based on the iterative integration of Newton's second law of motion for the DEM particles, the nodes of FEM triangular elements to update the contact forces, and the positions of the elements.

The soil/geotextile interaction is described by a contact law similar to that used in the DEM method between the grains. The relative displacement at the interface soil/geosynthetic is defined between the soil particle and the entire geosynthetic sheet to preserve the tangential friction history when a soil particle moves from one FEM sheet element to another.

4.2. Geometry and parameters selected for application to reinforced embankments over cavities

The numerical soil sample is constituted of particles of various shapes and sizes distributed randomly in a cylindrical box. Owing to the axisymmetric boundary conditions of the experimental device, and to save computational time, only a quarter of the cylindrical tank was considered (Fig. 3). A curved frictionless wall is used on the lateral sides to reproduce the boundary conditions. To control the density the numerical sample, a specific method (ERDF method, Salot et al. (2009)) based on the iterative growth of the particles radii and intergranular friction reduction was used. To reproduce the behavior of real granular materials (friction angle and dilatancy), the numerical samples were made using an assembly of particles with two spheres joined to each other by an unbreakable link. This choice of elongated grains in the simulations was based on the observation of the grain shape of the sand used experimentally. Two types of particles were used (Fig. 3) considering two juxtaposed spheres to simulate very elongated grains (model C1), or two interpenetrating spheres with a distance equal to the radius of particles to simulate less-elongated grains (model C2). The use of clumps (collection of spheres) would help simulate elongated grain shape by keeping simple contact detection and saving computational time. The numerical model parameters are calibrated so that the behavior of the numerical sample fits the friction characteristics determined through triaxial laboratory tests performed with the sand used in the experiments ($\Phi = 36.5^{\circ}$). Several samples with different initial porosities or grain shapes were tested so that the numerical samples mainly differed in their ability to expand during the opening of the cavity. Note that currently there are no standard tests that allow for a characterization of the expansion of the soil. The correlations between the macromechanical parameters of the numerical soils (friction angle Φ, dilatancy angle Ψ, and Young's modulus E), the micromechanical contact parameters (intergranular friction angle φ_c, and normal and tangential rigidities of the constitutive materials K_{nij} and K_{tij}), and the

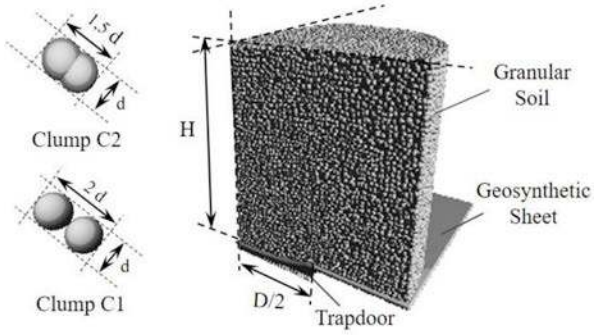

Fig. 3. Geometry of simulated samples and illustration of grain shapes used in simulation.

Table 1
Micro contact parameters [intergranular friction angle (φ_c), normal and tangential rigidities of the constitutive material [K_{nij}, K_{tij}], and macro parameters [friction angle at peak (Φ), dilatancy angle (Ψ), and Youngs modulus (E)] of the numerical soils used in the simulations.

Soil Type	Microparameters	Macroparameters	K_{nij}/Kt_{ij}	Φ	Ψ	$E(MPa)$
	φ_c	K_{nij} (MPa)				
C1P38	16.7°	100	1	36.5°	19°	16
C1P42	26.67°	100	1	36.5°	8°	16
C2P32	18°	100	1	36.5°	19°	16
C2P36	29.11°	100	1	36.5°	11°	16
C2P38	38°	100	1	36.5°	6°	16

numerical density and shape of the particles are listed in Table 1. In this table, the numerical soils are named as follows: C followed by the cluster type (1 or 2), and P followed by the value of the numerical porosity as a percentage.

The friction characteristics of the soil-geotextile interface were determined through laboratory tests on an inclined plane ($\delta = 25.44^{\circ}$ in the case of woven geotextile, and $\delta = 27.74^{\circ}$ when a nonwoven geotextile was used). The tests were performed following the recommendations of the European standard EN ISO 12957-2 (2005). The frictional interface of 0.48 m^2 (0.6 m in width and 0.8 m in length) makes it possible to conduct tests on geosynthetic samples of large dimensions. The upper box was filled with a 30 cm thick layer of soil as a load. In the absence of relative roughness between the geosynthetic sheet and the soil particles, the microscopic numerical friction angle of the interface can be considered equal to the macroscopic values indicated above. Similarly, the numerical stiffness values of the geotextile in the production and transverse directions were derived from those obtained via tensile laboratory tests (values given in the previous section). The numerical opening process of the cavity is simulated using underlying spheres placed under the geotextile. When a trapdoor opens, the spheres underlying the cavity are together slowly displaced downward. By contrast, during a progressive opening in the diameter, the underlying spheres are progressively removed from the center of the cavity toward its edge. Three different values of H/D were considered: $H/D = 0.5$, 1, and 1.5. The experimental diameter of the cavity was 0.50 m, which corresponded to an embankment height of 0.25, 0.50, and 0.75 m. The number of clusters (sphere assemblies: C1 or C2) used in the simulations were 30000, 60000, and 90000 for $H = 0.25$, 0.50 and 0.75 m, respectively. The simulation time vary depending on the number of grains, the cavity opening mode and the precision that was expected. For this study, the number of grains and the cavity opening velocity were adjusted to have reasonable computation durations on a personal computer (one week in research context).

5. Results: numerical-experimental comparison

The relevance of the numerical model was established in the following sections by comparison with the experimental results. Owing to the lack of experimental information related to the soil behavior (expansion coefficient or dilatancy in particular), and to determine the more suitable numerical model that represents well the soil behavior during the cavity opening, various numerical simulations with different particle shapes and various soil porosities were performed for $H/D = 0.5$. The more adequate grain geometry and skeleton porosity needed to reproduce the experimental test $H/D = 0.5$ were then adopted for all numerical simulations. The comparison between the experimental and numerical results were proposed (for various H/D values, different opening modes and several geotextile stiffnesses) in order to demonstrate the relevance of the numerical model and to improve the knowledge related to the load transfer mechanisms involved during the cavity opening. The numerical tests were named as

follows: Opening mode (T for trapdoor and P for progressive opening), geosynthetic type (W for woven and N for nonwoven), H followed by the value of the height of the embankment in cm, C followed by the type of clusters used (1 or 2), and P followed by the value of the numerical porosity as a percentage. A comparison was conducted based on the deflection of the geotextile and the surface settlement.

Considering the most adequate numerical soil model, a sensitivity parametric study was proposed to determine the influence of different parameters such as the grain shape, the initial porosity of the numerical sample, the thickness of the granular layer, the cavity-opening process, and the stiffness of the geosynthetic.

6. Influence of the grain shape and porosity of granular assembly on surface settlement, geosynthetic deflection, and load transfer mechanisms

This analysis was performed considering $H/D = 0.5$, a trapdoor-opening mode and a woven geotextile. Several numerical samples with different initial numerical porosities (32, 36, 38, and 42%) or variant grain shapes (C1 and C2) to determine the more adequate numerical model to reproduce the whole experimental phenomena. The influence of the geometrical soil characteristics on the load transfer mechanisms was also studied. In all cases tested, the numerical soil samples (Table 1) presented a peak friction angle of 36.5° but differed by various dilatancy angles. The deflection of the geotextile and the surface settlement were determined in both the machine and cross directions. The obtained curves were very similar in both directions, so the results were only plotted in one direction (the machine direction).

6.1. Geosynthetic deflection

Fig. 4 presents the results for the geosynthetic deflection *dg* as function of *R* the radius from the center of the cavity for the different types of simulated soil. The graph indicates that the deflection of the geosynthetic is slightly affected (around 10%) by the porosity and grain shape of the simulated soil. This is because the load transfer mechanisms are mainly governed by the macroscopic friction angle of the soils, which are similar for all tested numerical granular soils. For the same grain shape, the higher the porosity, the higher the value of the geotextile's deflection.

This was easily expected: the higher the density of the material (the lower the porosity), the higher the dilatancy of the material, and the higher the efficiency to transfer the load to the sides of the cavity, which leads to a lower geotextile deflection (*dg*). The shapes of the grains influence the deformations as well; the sample with more elongated grains (C1) was better able to develop load transfer mechanisms

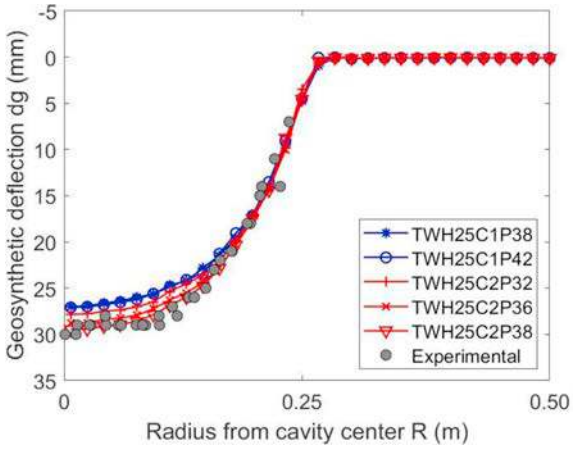

Fig. 4. Geosynthetic deflection for various soil properties when H/D = 0.5, for woven geosynthetic and trapdoor opening process.

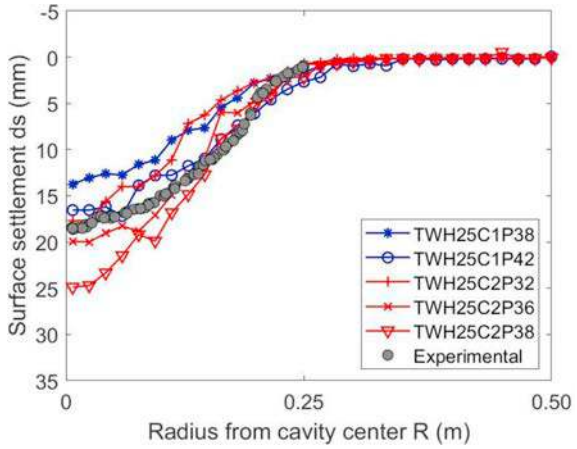

Fig. 5. Surface settlement for various soil properties when H/D = 0.5 for woven geosynthetic and trapdoor opening process.

which led to lower geotextile deflection. However, the differences between the values of the maximum deflection of the different simulated soils remain small (smaller than the value of the experimental accuracy (± 2.5 mm)).

6.2. Surface settlement

Fig. 5 presents the results for the surface settlement *ds* for the different types of simulated soils in the case of a trapdoor opening, woven geotextile, and a ratio of $H/D = 0.5$. The figure shows that the surface settlements are more affected than the geotextile deflections by the soil properties. In fact, as mentioned previously, the higher the dilatancy of the material (lower porosity or more elongated grains), the better the ability of the material to expand. Considering rather similar deflections of the geosynthetic, this leads to lower surface settlements (*ds*). Notice that if the surface settlement curves are compared to the experimental ones, several soil types seem very suitable for describing the expansion behavior of the soil tested experimentally, with a maximum surface settlement difference that remains smaller than the experimental accuracy of ± 1.5 mm. Considering that the sample characterized by the C2 grain shape and a 36% porosity is one of the more adequate numerical materials that allows for the fit of both geosynthetic and surface settlements, it was retained for a parametric sensitivity study. Moreover, to be sure that the number of clusters chosen for the simulation is sufficient, the numerical simulation TWH25C2P36 was also repeated by increasing the number of clusters to 60000 to compare it to the previous numerical simulation with 30000 clusters. As can be seen in Table 2, the results in terms of the surface settlement and geosynthetic deflection are the same, thus validating the number of 30000 clusters for $H/D = 0.5$.

6.3. Analysis of expansion mechanisms as function of grain shape or initial material density

The value of the expansion coefficient needed in the analytical design method of the reinforcement over the cavity is always an open question owing to the difficulty that remains in its experimental determination. One interesting issue with the numerical DEM model is its

Table 2
Maximum geotextile deflection and surface settlement for different numbers of clusters.

Test	Number of clusters	*dg* (*mm*)	*ds* (*mm*)
TWH25C2P36	30000	28.7772	19.9252
TWH25C2P36	60000	28.7778	19.9250

ability to analyze the expansion phenomenon by considering the increase or decrease in volume of any part of the granular sample. Two numerical ways to calculate the expansion of the soil can be used: the determination of an average expansion coefficient within the cylinder of soil sited above the cavity or the calculation of several local values of the expansion coefficient within different horizontal cylindrical layers sited at various heights. The expansion coefficient in a fixed zone is calculated as the ratio of the expanded soil volume over the initial one.

$$C_e = \frac{V_f}{V_i} \tag{6}$$

The initial and final volumes of a fixed zone are calculated by meshing the granular sample and detecting the positions of the grains on the upper and lower borders. Taking into consideration the new positions of these grains after the cavity-opening process, the expanded soil volume can be determined. This method is mesh and grain-size dependent. The uncertainty on the calculated value of the expansion coefficient due to this numerical process was estimated by comparing the initial volume of the soil embankment above the cavity (determined numerically before the cavity opening) to the theoretical volume of a cylinder having the cavity size. Several mesh sizes were tested, and the mesh with the minimum error value was retained. The minimum obtained error was about 2%.

Fig. 6 shows the influence of the numerical sample porosity on the average expansion coefficient calculated numerically above the cavity for soil type C2, in the case of a trapdoor opening process and $H/D = 0.5$. Considering that all numerical samples tested had the same macroscopic peak friction angle, this comparison mainly reflects the influence of the change in geometry and density of the granular skeleton. It is noticed in Fig. 6 that the higher the density, the lower the porosity and the higher the global expansion coefficient C_e.

For a better understanding of the expansion phenomenon within the granular layer, the local expansion coefficient and local porosity are calculated and then averaged on horizontal layers at different heights of the soil cylinder above the cavity. Fig. 7 shows the evolution of the local expansion coefficient as a function of the height and shows that C_e is not uniform within the granular embankment sited over the cavity. It is noticed that C_e decreases rather linearly with the depth of the embankment (for all performed numerical simulations). Similarly, the consecutive change in porosity to the cavity-opening process follows the same trend (Fig. 8). The initial porosity is rather uniform within the embankment. At the end of the opening process, the mean value of the porosity in each horizontal layer increases owing to the expansion of the soil, but the increase is more important close to the surface for which the confining pressure is null.

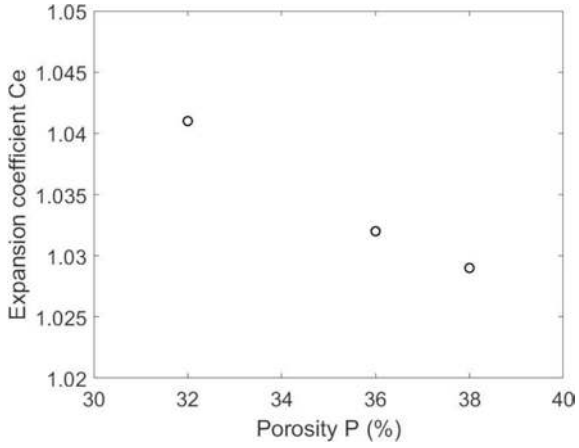

Fig. 6. Global expansion coefficient values for different initial porosity values of samples, for soil type C2, woven geosynthetic, trapdoor opening and H/D = 0.50.

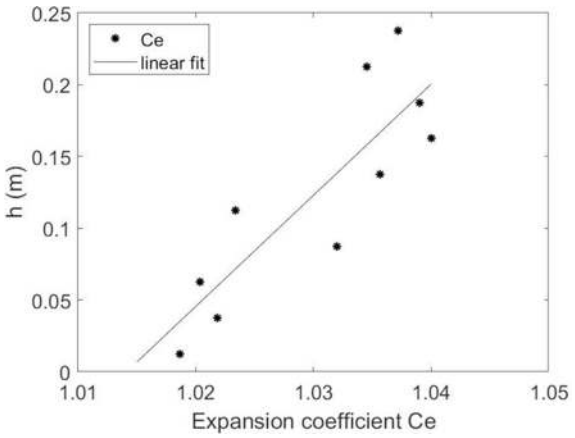

Fig. 7. Evolution of expansion coefficient with height of embankment over cavity for soil C2P36, woven geosynthetic, trapdoor opening and H/D = 0.50 (H = 0.25 m).

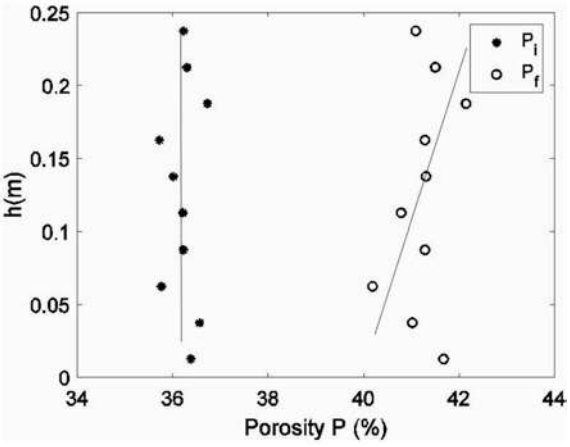

Fig. 8. Evolution of initial and final porosity with height of embankment over cavity, for soil C2P36, woven geosynthetic, trapdoor opening and H/D = 0.50.

6.4. Analysis of efficiency of load transfer as function of initial granular density

The load transfer efficiency reflects the ability of a granular material to allow for the reorganization of the contact force network consecutively based on a change in the boundary conditions. These load transfer mechanisms are influenced by the macroscopic friction angle of the granular material, the shape of the grains, and the geometry of the granular skeleton (density state). The load transfer within the granular embankment can be characterized by the efficiency, defined as the ratio between the parts of the vertical load reported toward the edges of the cavity ΔQ over the weight of the cylindrical soil volume sited above the cavity W_s. ΔQ can be computed either by considering the charge drop over the cavity or by the increase in charge on the sides.

$$E = \Delta Q / W_s \tag{7}$$

Table 3 lists the values of efficiency obtained considering different values of porosities. It can be seen that the efficiency increases slightly with the density. As mentioned before, all numerical samples tested have the same macroscopic peak friction angle, so that this comparison reflects exclusively the influence of the geometry of the granular assembly. This explains why the increase in efficiency is not so important.

7. Sensitivity analysis of influence of embankment height

A sensitivity analysis performed for different H/D ratios was carried

Table 3
Efficiency values of tests with C2 grain shape for various initial porosity values.

Test	Efficiency (%)
TWH25C2P32	42
TWH25C2P36	37
TWH25C2P38	34

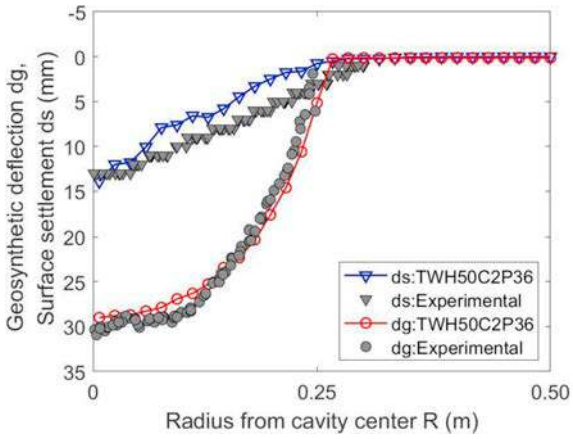

Fig. 9. Surface settlement and geotextile deflection for test TWH50C2P36 when P = 0.36 and H/D = 1 for woven geosynthetic and trapdoor opening process.

out with the numerical granular material selected previously that fits the best experimental results obtained for $H/D = 0.5$: a sample with C2 grain shape and 36% porosity. A comparison with the experimental results and an analysis of the load transfer mechanisms were conducted.

7.1. Surface settlement and geosynthetic deflection

Figs. 9 and 10 present a comparison between the numerical and experimental results of geosynthetic deflection and surface settlement for different embankment heights. As can be seen, the numerical model reproduces well the curvature of the geotextile's deflection and that of the surface settlement. It is also possible to estimate the value of the experimental maximum surface settlement with accuracy of ± 1.5 mm and the experimental maximum geosynthetic deflection with accuracy of ± 2 mm. This is equal to or lowers than the experimental accuracy.

One point that needs to be emphasized is the fact that the experimental values of the vertical displacements of the geosynthetic are

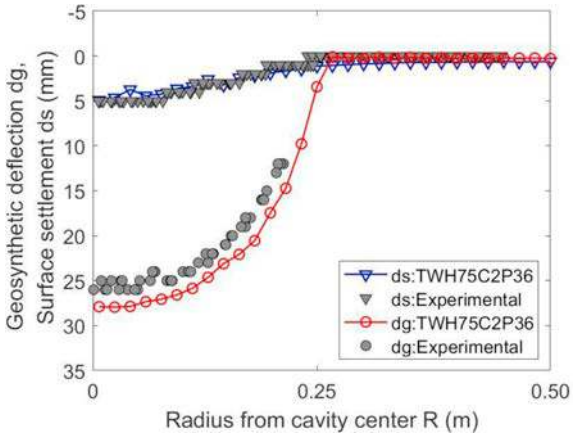

Fig. 10. Surface settlement and geotextile deflection for test TWH75C2P36 when P = 0.36, H/D = 1.5 for woven geosynthetic and trapdoor opening process.

Table 4
Global Expansion coefficient values for different embankment heights.

Test	C_{eexp}	C_e
TWH25C2P36	1.026	1.032
TWH50C2P36	1.024	1.027
TWH75C2P36	1.020	1.017

rather similar for the studied thicknesses of the granular soil layers. The numerical model confirms these results. To explain this, note that a large thickness of the granular layer is more able to prone the load transfer mechanisms. This is demonstrated later by an analysis of the load transfer efficiency.

Another point that needs also to be emphasized is the decrease in the surface settlement with an increase in embankment thickness. This can be easily explained considering that the volume of soil able to expand during the cavity-opening process is a linear function of the embankment height, and that the deflections of the geosynthetic are rather similar from one case to another.

7.2. Expansion coefficient

The average numerical expansion coefficients were determined considering the cylindrical volume of soil sited above the cavity. Table 4 compares the values of the global expansion coefficients obtained from the laboratory experiments C_{eexp} (Pham et al. (2017)) and the values of those obtained numerically C_e for various H/D ratios. It is noticed that the numerical model predicts the global expansion coefficient of the soil over the cavity with an error less than 2%, and that C_e decreases when H/D increases. This is of major importance when using this coefficient in analytical design methods. This can be explained as follows:

— Greater grain confining pressures in the case of high-thickness embankments that counteract the expansion phenomenon.
— Lower shear strain rates (ratio between the maximal displacement of the granular embankment vs. its height) for high-thickness embankments.

7.3. Efficiency of load transfer

Table 5 presents the values of efficiency for different embankment heights. As mentioned previously, the load transfer efficiency increases with an increase in the H/D ratio. This indicates that the thickness of the embankment significantly influences the load transfer mechanism.

These results agree with the values of efficiency found in Villard et al. (2016).

However, the values of efficiency obtained numerically are higher than the values obtained experimentally by Pham et al. (2018) but are in accordance with the values of the vertical deflection of the geotextile. This discrepancy with the experimental results may be attributed to the difficulties encountered when estimating the experimental vertical load acting on the geosynthetic sheet due to the limitations of the tactile pressure sensor used in the measurements of stress. It can be noted that depending on the case, a large amount of the weight of the cylinder of soil sited over the cavity is transferred at the side of the cavity (around 37–76% for the studied cases). The influence of the height of the

Table 5
Efficiency values of tests for different embankment heights.

Test	Efficiency (%)	Efficiency_{exp} (%)
TWH25C2P36	37	25
TWH50C2P36	63	30
TWH75C2P36	76	32

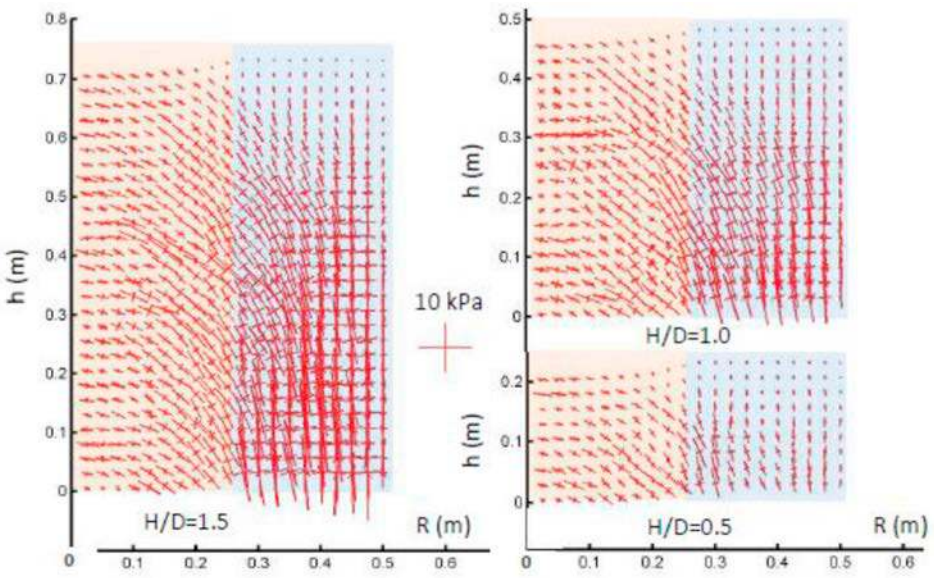

Fig. 11. Principal stresses within granular embankment for different H/D ratios, soil C2P36, woven geosynthetic and trapdoor opening.

embankment on the load transfer mechanisms (seen as a change in the principal stress orientation) is also shown in Fig. 11. The figure shows the principal stress tensors. Very different arching mechanisms can be observed for different H/D ratios.

8. Sensitivity analysis of influence of opening mode

To compare with the previous results involving a trapdoor opening process, new numerical simulations were carried out using the numerical granular material selected previously (numerical granular material C2P36) and considering a progressive cavity-opening process by increasing the cavity diameter. The results of the progressive cavity-opening process were first compared with the experimental ones. Then, the load transfer phenomena, in terms of the vertical load distribution acting on the geosynthetic, and of the shearing mechanisms within the granular embankment, were numerically investigated for both opening processes.

8.1. Comparison with experimental results

The results in terms of the geosynthetic vertical displacements and of the surface settlements, obtained considering the progressive opening mode by increasing the cavity diameter, are compared to the experimental ones in Fig. 12. In this figure, it can be seen that the DEM numerical model again predicts very well the experimental data with good accuracy. It can be also emphasized that, in this case, the geotextile deflection and the surface settlement are much higher than the values of the displacement obtained for a trapdoor opening. This reflects a change in the load transfer mechanisms depending on the cavity-opening mode. This will be discussed later. A comparison between the experimental global expansion coefficient and that obtained considering the numerical progressive opening mode demonstrates the relevance of the numerical model (C_e = 1.049 and C_{eexp} = 1.033). In addition, a comparison of the average global expansion coefficient for the two opening processes (C_e = 1.032 for a trapdoor opening and C_e = 1.049 for a progressive opening) indicates a significant difference in the expansion mechanisms within the granular embankments as a function of the kinematics of the opening process.

Comparing the efficiency of both opening modes (37% for the trapdoor opening vs. 45% for the progressive opening mode), it is noticed that the efficiency is slightly higher for the progressive opening mode when H/D = 0.5. In addition, it was mentioned by Villard et al. (2016) that the opening mode does not have a great influence on the efficiency values when H/D = 0.5.

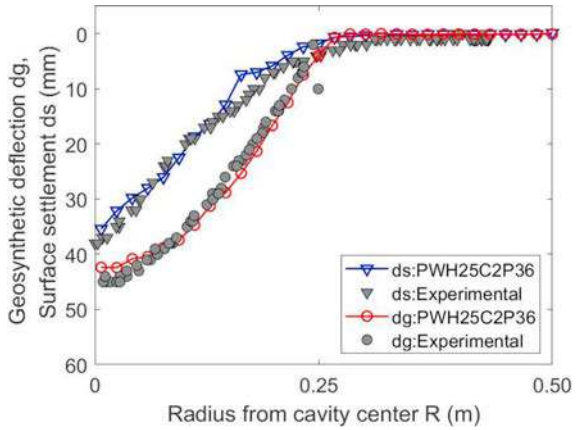

Fig. 12. Surface settlement for test PWH25C2P36 when P = 0.36 and H/D = 0.5 for woven geosynthetic and progressive opening process.

8.2. Comparison of numerical vertical load distribution acting on geosynthetic sheet

To better understand the influence of the cavity-opening modes on the load transfer mechanisms, and to explain the difference in the geotextile deflection between one process and another, the vertical load distributions acting on the geosynthetic sheet were investigated via the vertical contact forces that can be calculated between the soil particles and the geosynthetic sheet. Considering these contact forces, the vertical stresses are determined on annular areas centered on the center of the cavity.

The changes in the vertical stresses acting on the geotextile ($\Delta\sigma/\sigma_0 = (\sigma_f - \sigma_0)/\sigma_0$), where σ_0 is the stress acting on the geotextile before the opening of the cavity and σ_f the stress at the end of the opening process, are presented for both opening processes (Fig. 13). It is noticed that for the trapdoor opening process, the stress distribution is higher around the cavity and is almost constant in the central part, while it has a conical shape in the case of a progressive cavity opening (Fig. 13). An increase in the stress on the edges of the cavity and on the borders owing to the arching effect is also clearly observed. These results agree

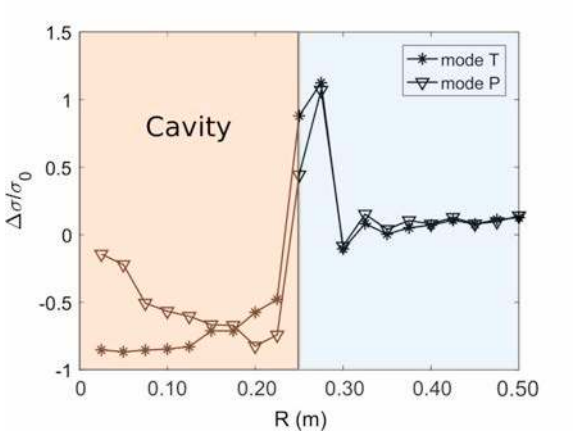

Fig. 13. Changes in stresses on geosynthetic sheet, for soil C2P36, woven geosynthetic and H/D = 0.50.

with the results published by Villard et al. (2016) and with the general tendencies from the experimental studies of Pham et al. (2018).

8.3. Comparison of numerical shearing mechanisms within granular embankment

This section discusses the load transfer mechanism acting within the granular embankment in terms of shearing stresses for the different opening modes of the cavity. In fact, when the cavity opens, relative displacements will occur between different parts of the soil, developing more or less large shear bands. Stress will also be transferred from the yielding soil to the adjacent zones. This is known as the arching effect. This means that by looking at the shear stresses within the granular embankment and their evolution, the load transfer mechanisms can be also tracked.

For this, the granular embankment is meshed into elementary cubes where the stress tensor is calculated. During the opening process, the intensity and position from the cavity center of the maximum shear stress can be tracked.

Fig. 14 depicts the evolution in intensity and position of the maximum shear stress value during both trapdoor and progressive opening tests. The arrow indicates the evolution of the intensity and position of the maximum sheared zone with the opening of the cavity.

Fig. 14 shows that the shearing process is quite different for both opening modes. In the case of a trapdoor opening, the most sheared zone is located at the cavity border at the beginning of the opening process and moves toward the center of the cavity with an increase in trapdoor displacement, thus promoting the load transfer. In fact, in the trapdoor process, the contact between the geosynthetic and the trapdoor is progressively lost from the border of the cavity to its center. This leads at the end of the opening process to a higher value of the shearing stress at the center of the cavity. This explains why the vertical load acting on the central part of the cavity at the end of the opening process is smaller than that observed on the border. In the case of a progressive opening by an increase in diameter, the opposite mechanism takes place. The maximum shear stress value is first located in the center of the cavity and moves toward the borders. The maximum stress value decreases during the opening process. This indicates that a certain amount of soil is already acting on the sheet, leading to the conical shape of load distribution that was obtained previously.

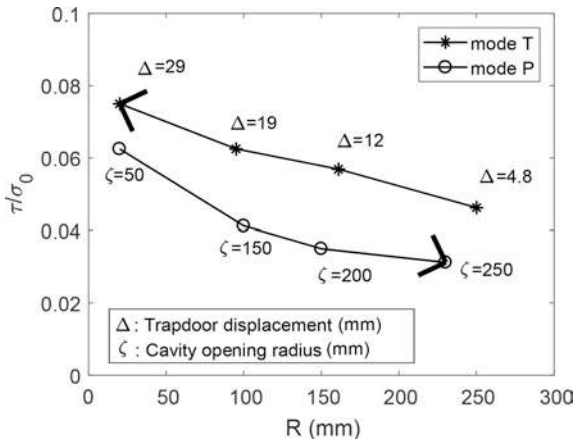

Fig. 14. Evolution of shearing for both opening modes, for soil C2P36, woven geosynthetic and H/D = 0.50.

9. Influence of geotextile stiffness

The influence of the stiffness of the geotextile could be investigated by comparing the previous results presented section 6 (woven geotextile- Machine-direction stiffness: 160 kN/m; Cross-direction stiffness: 160 kN/m) to the experimental and numerical results presented in this section involving a nonwoven geotextile (Machine-direction stiffness: 9.21 kN/m; Cross-direction stiffness: 8.75 kN/m) for the case $H/D = 0.5$. The stiffness of the nonwoven geotextile is much lower than the stiffness of the woven geotextile. Thus, greater deformations of both the granular embankment and geosynthetic sheet were expected. Owing to large displacements of the granular embankment, the surface settlement is more sensitive to the expansion coefficient of the soil. Thus, various numerical simulations implying different particle shapes and various soil porosities were performed in the case on the nonwoven geotextile as made previously. A comparison with the results presented in section 6, when a woven geotextile was used, was made based on the deflection of the geotextile, the surface settlement, the expansion coefficient, and the efficiency of the load transfer.

9.1. Geotextile deflection and surface settlement

Fig. 15 presents the geotextile deflection for several numerical soils when a nonwoven geotextile is used. The results show that the soil (C2P36) that was selected previously when a woven geotextile was used, leads to greater vertical displacements than those deduced from the experiment. By contrast, the other soils tested seem rather relevant when predicting the deflection of the geosynthetic sheet in the case of woven geotextile. By plotting the surface settlement for the different numerical soils, It can be concluded that the soils with C1 grain type that were the most adapted to expand during shearing are the numerical soils that best reflect reality. In fact, looking at all results presented

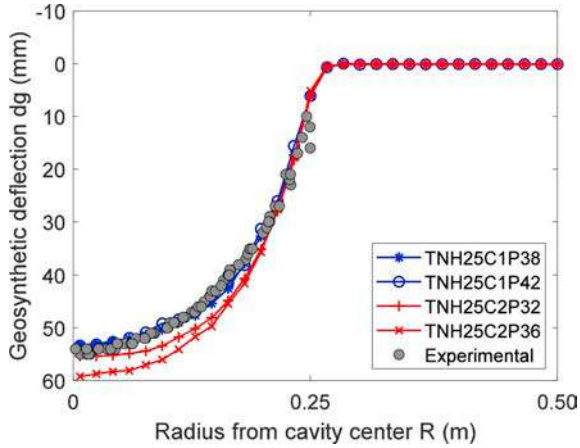

Fig. 15. Geosynthetic deflection for various soil properties when H/D = 0.5 for nonwoven geosynthetic and trapdoor opening process.

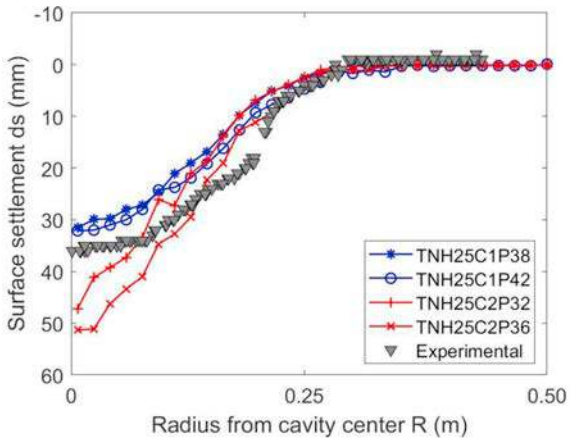

Fig. 16. Surface settlement for various soil properties when H/D = 0.5 for nonwoven geosynthetic and trapdoor opening process.

for woven in section 6 (Figs. 4 and 5) and nonwoven geotextiles (Figs. 15 and 16), the results obtained for soil C1P42 seem to be the most suitable to represent with a very good accuracy the load transfer mechanisms and the expansion phenomenon of the real soil.

9.2. Expansion coefficient and efficiency of load transfer

The influence of the tensile stiffness of the geosynthetic sheet on the soil expansion coefficient and the efficiency of the load transfer were both analyzed. The numerical expansion coefficient values (C_e = 1.034 for C1P38 and C_e = 1.027 for C1P42) also fit well with the experimental value (C_e = 1.033). These numerical expansion coefficient values were also very close to the numerical values obtained in the case of woven geotextile (C_e = 1.032). These results, valid for H/D = 0.5, may be different considering different ratios H/D or different tensile stiffnesses.

The numerical values of the efficiency (30% for C1P38 and 28% for C1P42) in the case of nonwoven geotextile are slightly lower than the numerical values in the case of woven geotextile (37%). A lower load is transferred to the border of the cavity; this might be due to the fact that the granular embankment is subjected to higher deformations, leading to smaller shearing stress when the stiffness of the geotextile is lower.

10. Conclusions and perspectives

A numerical model based on DEM and FEM coupling is used to reproduce laboratory experiments performed by Pham et al. (2018) which consist on cavities opening under granular embankments reinforced by geosynthetic sheet. These numerical and experimental coupled studies allowed to highlight the complex mechanisms developed within the reinforced mattress over the cavity. The numerical and experimental results of the surface settlement of the embankment, the geosynthetic deflection, and the global expansion coefficient over the cavity area (which was generally not estimated in practice) are compared for three different heights of granular embankment (H/D = 0.5,1,1.5), two cavity-opening modes (trapdoor and progressive) and different geotextile stiffnesses (woven and nonwoven). It appears that, for the cases presented in this study, the numerical model is a relevant tool to analyze the load transfer mechanisms within the granular embankment and to predict the reinforced embankment behavior. Its main advantage is its ability to provide extra microscopic information at the grain level that is difficult to measure experimentally such as: local deformations, grain displacements, the network of contact forces and stress distribution within the granular mattress as it is presented in this work. The numerical tool also allows performing sensibility analysis by varying only one soil characteristic (for example, by varying the grain shape or the soil density while keeping constant the macroscopic peak friction angle). From this, the influences of the cavity-opening mode, the height of the embankment, the geosynthetic stiffness, and the soil geometrical characteristics were investigated.

The sensitivity analysis implying numerical soils of different densities and grain shapes highlights the influence of soil properties on the load transfer mechanisms. For a given embankment height, it can be concluded that soil geometrical characteristics mainly affect the surface settlement values owing to different expansion phenomena, while the geosynthetic deflection remains slightly affected. The numerical results also confirm that the vertical displacements of the geosynthetic are rather similar for the studied thicknesses of the granular soil layers because a higher embankment is more able to prone the load transfer mechanisms. As expected, the surface settlement and geosynthetic deflection are functions of the geosynthetic tensile stiffness.

From the sensitivity analysis, it was also shown that the local expansion coefficient over the cavity is not uniform over the depth of the embankment and depends on the cavity-opening mode, grain shape, soil density, shear strain rate, and height of the embankment. It can be emphasized that this is now not considered in current design methods. Numerical values between 1.03 and 1.045 were obtained. The efficiency of the load transfer depends on many parameters. The most influential parameter is the height of the embankment, which leads to very different arching mechanisms. Efficiencies between 37 and 76% were obtained for H/D ratios varying between 0.5 and 1.5.

The stress distribution on the geotextile sheet is presented for both cavity-opening modes. The obtained stress profiles confirm previous numerical studies showing that the stress is not uniform over the cavity, as is commonly considered in most existing design methods.

The shear stress within the granular embankment is also computed in this paper, and the results show that the direction of shearing for both opening modes is not the same. While shearing progresses from the cavity center to its borders for progressive openings, it progresses from the borders toward the center in the trapdoor-opening mode, which explains the load distribution acting on the geotextile sheet for different opening modes.

Finally, further investigations are needed to better understand the load transfer mechanisms involved in more complex loading cases and improve the design methods. Extra simulations can be done to link the expansion coefficient and the efficiency parameter to the opening mode, H/D ratio, and soil properties (e.g., density, grain size distribution, and friction angle).

Acknowledgment

This study was performed in the framework of the new French laboratory PITAGOR (Laboratory of Technical Innovations Applied to Reinforcement Geosynthetics) and was funded in December 2015 by the French National Research Agency. It associates with the research laboratory GEOMAS and the geosynthetic producer TEXINOV.

References

Alexiew, D.A., 1997. Bridging a sink-hole by high-strength high modulus geogrids. In: Proceedings of the Geosynthetics' 97 Conference, Long Beach, Calif., U.S.A, vol. 1. Industrial Fabrics Association International (IFAI), St. Paul, MN, pp. 13–24.

Blivet, J., Khay, M., Villard, P., Gourc, J., 2000. Design method for geosynthetic as reinforcement for embankment subjected to localized sinkholes. In: GeoEng2000, International Conference on Geotechnical and Geological Engineering, Melbourne, Austria, pp. 1–6.

Briançon, L., Nancey, A., Caquel, F., Villard, P., 2004. New technology for strain measurements in soil and the survey of reinforced earth constructions. Proceedings of EUROGEO 3, 1–3.

Briançon, L., Nancey, A., Villard, P., 2005. Development of geodetect: a new warning system for the survey of reinforced earth constructions. Studia Geotechnica Mech. 27 (1–2), 21–32.

Briancon, L., Villard, P., 2008. Design of geosynthetic-reinforced platforms spanning localized sinkholes. Geotext. Geomembranes 26 (5), 416–428.

British Standard, B., 2010. Standards Publication Code of Practice for Strengthened/

reinforced Soils and Other Fills. pp. 1–21 ISBN 940005429.
Chareyre, B., Villard, P., 2005. Dynamic spar elements and discrete element methods in two dimensions for the modeling of soil-inclusion problems. J. Eng. Mech. 131 (7), 689–698.
Chen, C., McDowell, G., Thom, N., 2012. Discrete element modelling of cyclic loads of geogrid-reinforced ballast under confined and unconfined conditions. Geotext. Geomembranes 35, 76–86.
Cundall, P.A., Strack, O.D., 1979. A discrete numerical model for granular assemblies. Geotechnique 29 (1), 47–65.
Donzé, F.V., Magnier, S.A., 1995. Formulation of a three dimensional numerical model of brittle behavior. Geophys. J. Int. 122, 790–802.
EBGEO, 2010. die berechnung von erdkörpern mit bewehrungen aus geokunststoffen-ebgeo, deutsche gesellschaft für geotechnik ev (dggt), vol. 2.
EN ISO 12957-2, 2005. Geosynthetic - Determination of Friction Characteristics, Part 2: Inclined Plane Test. European Committee for Standardization, Brussels.
Feng, S.J., Ai, S.G., Chen, H.X., 2017. Estimation of arching effect in geosynthetic-reinforced structures. Comput. Geotech. 87, 188–197.
Giroud, J., 1995. Determination of geosynthetic strain due to deflection. Geosynth. Int. 2 (3), 635–641.
Kinney, T.C., 1986. Reinforced roads bridging voids. In: Cold Regions Engineering: ASCE, pp. 320–329.
Kinney, T.C., Connor, B., 1987. Geosynthetics supporting embankments over voids. J. Cold Reg. Eng. 1 (4), 158–170.
Kinney, T., Connor, B., 1990. Geosynthetic reinforcement of paved road embankments on polygonal ground. J. Cold Reg. Eng. 4 (2), 102–112.
Le Hello, B., 2007. Renforcement par géosynthétiques des remblais sur inclusions rigides, étude expérimentale en vraie grandeur et analyse numérique. Ph.D. thesis. Université Joseph-Fourier-Grenoble I.
McDowell, G., Harireche, O., Konietzky, H., Brown, S., Thom, N., 2006. Discrete element modelling of geogrid reinforced aggregates. Proceedings of the Institution of Civil Engineers-Geotechnical Engineering 159 (1), 35–48.
Pham, M.T., Briançon, L., Dias, D., Abdelouhab, A., 2017. Etude expérimentale des mécanismes de déformation développés dans les plateformes granulaires renforcées par géosynthétiques sur cavités. In: Proceedings of the 19th International Conference on Soil Mechanics and Geotechnical Engineering, Seoul.
Pham, M.-T., Briançon, L., Dias, D., Abdelouhab, A., 2018. Investigation of load transfer mechanisms in granular platforms reinforced by geosynthetics above cavities. Geotext. Geomembranes 46 (2018), 611–624.
Rui, R., Van Tol, A.F., Xia, Y.Y., Van Eekelen, S.J.M., Hu, G., 2016. Investigation of soil-arching development in dense sand by 2D model tests. Geotech. Test J. 39 (3), 415–430.
Salot, C., Gotteland, P., Villard, P., 2009. Inuence of relative density on granular materials behavior: dem simulations of triaxial tests. Granul. Matter 11 (4), 221–236.
Schwerdt, S., MEXER, N., Paul, A., 2004a. Die bemessung von geokunststo_bewehrungen zur ueberbrueckung von erdeinbruechen (bge-verfahren)/the design of geosynthetic reinforcements for protection against surface collapse into underground voids. Bauingenieur 79 (9).
Schwerdt, S., Naciri, O., Jenner, C., 2004b. Performance of aggregates in geogrid-reinforced soils used for protection against surface collapse into underground voids. In: EuroGeo 3: Geosyntetics Conference, pp. 483–488.
Terzaghi, K., 1943. Theoretical Soil Mechanics. john wiley & sons, new york.
Villard, P., Giraud, H., 1998. Three-dimensional modeling of the behavior of geotextile sheets as membranes. Textil. Res. J. 68 (11), 797–806.
Villard, P., Gourc, J., Giraud, H., 2000. A geosynthetic reinforcement solution to prevent the formation of localized sinkholes. Can. Geotech. J. 37 (5), 987–999.
Villard, P., Briancon, L., 2008. Design of geosynthetic reinforcements for platforms subjected to localized sinkholes. Can. Geotech. J. 45 (2), 196–209.
Villard, P., Chevalier, B., Le Hello, B., Combe, G., 2009. Coupling between finite and discrete element methods for the modelling of earth structures reinforced by geosynthetic. Comput. Geotech. 36 (5), 709–717.
Villard, P., Huckert, A., Briançon, L., 2016. Load transfer mechanisms in geotextile-reinforced embankments overlying voids: numerical approach and design. Geotext. Geomembranes 44 (3), 381–395.

Nomenclature

α: k_t/k_n
δ: Friction angle of the interface soil-geotextile
Φ: Friction angle of the granular soil
φ_c: Intergranular friction angle
Ψ: Dilatancy angle of the granular soil
ρ: Soil density
σ_f: Final vertical stresses acting on the geotextile
σ_0: Initial vertical stresses acting on the geotextile
τ: Maximum shear stress
C_e: Expansion coefficient determined numerically
C_{eexp}: Expansion coefficient determined experimentally
D: Cavity diameter
Dg: Geosynthetic deflection
ds: Surface settlement
E: Efficiency of load transfer
E: Young's modulus of the granular soil
F_e: Elementary force for each thread direction
F_n: Normal component of the contact force between two grains
F_t: Tangential component of the contact force between two grains
H: Granular embankment height
K_e: Elementary rigidity matrix characteristic of one thread direction
k_n: Normal contact stiffness
k_t: Tangential contact stiffness
K_{nij}: Normal rigidity of the two constitutive materials of the spheres i and j in contact
K_{tij}: Tangential rigidity of the two constitutive materials of the spheres i and j in contact
P: Porosity of the granular soil
Q: Load acting on the cylindrical soil above the cavity
R: Radius from the center of the cavity
R_e: Vector taking into consideration high displacements
R_i: Radius of grain (sphere) i
u: Normal overlap between two grains
u_e: Nodal displacement vector
v: Tangential displacement between two grains
V_f: Expanded soil volume over the cavity after cavity opening
V_i: Initial soil volume over the cavity
W_s: Weight of the cylindrical soil above the cavity